JBC RESEARCH ARTICLE

Prmt5 promotes ciliated cell specification of airway epithelial progenitors *via* transcriptional inhibition of Tp63

Received for publication, January 25, 2023, and in revised form, June 16, 2023 Published, Papers in Press, June 24, 2023,
https://doi.org/10.1016/j.jbc.2023.104964

Qiuling Li[1,*,‡], **Jie Jiao**[2,‡], **Ya Heng**[1], **Qingshuang Lu**[1], **Yu Zheng**[2], **Huijun Li**[2], **Jun Cai**[3], **Mei Mei**[2], **and Shilai Bao**[2,4,*]

From the [1]*Institute of Health Sciences and Technology, Institutes of Physical Science and Information Technology, Anhui University, Hefei, China;* [2]*State Key Laboratory of Molecular Developmental Biology, Institute of Genetics and Developmental Biology, The Innovative Academy of Seed Design, Chinese Academy of Sciences, Beijing, China;* [3]*Key Laboratory of Genomic and Precision Medicine, Beijing Institute of Genomics, Chinese Academy of Sciences, Beijing, China;* [4]*Department of Hematology Oncology Center, Beijing Children's Hospital, Capital Medical University, Beijing, China*

Reviewed by members of the JBC Editorial Board. Edited by Phillip A. Cole

The epithelium of the pulmonary airway is composed of several distinct cell types that differentiate from common progenitor cells to provide defense against environmental insults. Epigenetic mechanisms regulating lineage differentiation of airway epithelial progenitors remain poorly understood. Protein arginine methyltransferase 5 (Prmt5) is a predominant type II arginine methyltransferase that methylates >85% of symmetric arginine residues. Here, we provide evidence for the function of Prmt5 in promoting ciliated cell fate specification of airway epithelial progenitors. We show that lung epithelial-specific deletion of *Prmt5* resulted in a complete loss of ciliated cells, an increased number of basal cells, and ectopic-expressed Tp63^{-}Krt5^{+} putative cells in the proximal airway. We further identified that transcription factor Tp63 is a direct target of Prmt5, and Prmt5 inhibited Tp63 transcription expression through H4R3 symmetric dimethylation (H4R3sme2). Moreover, inhibition of Tp63 expression in *Prmt5*-deficient tracheal progenitors could partially restore the ciliated cell deficient phenotype. Together, our data support a model where Prmt5-mediated H4R3sme2 represses *Tp63* expression to promote ciliated cell fate specification of airway progenitors.

The airway epithelium is the first barrier of defense of the respiratory system against invading pathogens and inhaled particles from the environment. It is a pseudostratified epithelial structure composed of multiple cell types arranged in luminal and basal layers (1). The luminal layer is populated by secretory cells (club cells) and multiciliated cells (ciliated cells), and a small number of rare and special cell types, including neuroendocrine cells, goblet cells, brush cells (tuft cells), and ionocytes (2–4). The basal layer is populated by transformation-related protein 63 (Trp63, Tp63) and keratin 5 (Krt5)-expressing basal cells (5). Each type of airway epithelial cell performs designated roles. Aberrant cell type proportions and functions are often associated with human respiratory diseases, such as pulmonary inflammation, bronchopulmonary dysplasia, chronic obstructive pulmonary disease, and asthma (6).

Ciliated cells are terminally differentiated cells that occupy approximately half of the luminal layer of conducting airways. The main function of ciliated cells is to shuttle inhaled particulates and microorganisms, which were trapped by mucus-producing secretory and goblet cells, out of the airways by swinging the cilia on its apical surface in a retrograde manner (1). During lung development, ciliated cells are derived from a population of multipotent endodermal progenitors known to express transcriptional factor Myb to initiate ciliated cell fate specification (7), and inhibition of Notch signaling in airway progenitors is also required. It was well demonstrated that activation of Notch signaling in airway progenitor cells leads to secretory cell differentiation, while inhibition of Notch singling leads to ciliated cell differentiation (8, 9). Studies on molecular and genetic mechanisms have identified multiple factors that regulate ciliated cell specification and subsequent ciliogenesis, including serine/threonine kinase STK11 (10), E3 ubiquitin ligase FBXW7 (11), as well as a variety of transcription factors (Sox2, E2F4, Sox21, Foxj1, Nkx2-1, Tp63, Tp73, Myb, and Sox9) (12–16). However, little is known about the roles and mechanisms of epigenetic factors during ciliated cell fate specification and ciliogenesis.

Protein arginine methyltransferase 5 (Prmt5) is a type II protein arginine methyltransferase that catalyzes the symmetric dimethylation of arginine residues of histone or non-histone substrates, and therefore regulates the expression of target genes through epigenetic mechanisms (17). It has been reported that Prmt5 plays an important role in DNA repair, cell proliferation, transcriptional regulation, and spliceosome assembly (18–22). In mice, deletion of *Prmt5* prevents pluripotent cells to form the inner cell mass and leads to embryonic lethality (23). Pieces of evidence collected from conditional *Prmt5* KO mice suggest that Prmt5 participates in several stem/progenitor cell proliferation processes such as lung epithelial progenitor cells, hematopoietic stem cells and muscle stem cells (24–26). Prmt5 is also essential for the maintenance of neural stem/progenitor cells and spermatogonial stem cells (27, 28). In contrast, Prmt5 is not required for

‡ These authors contributed equally to this work.
* For correspondence: Qiuling Li, qlli@ahu.edu.cn; Shilai Bao, slbao@genetics.ac.cn.

primordial germ cell specification in mice (29). Although the necessity of Prmt5 in stem/progenitor cell maintenance and specification is therefore well-documented, it remains unclear whether Prmt5 is required for airway stem/progenitor cells to differentiate into specific cell types.

In the present study, we show that lung epithelial-specific deletion of *Prmt5* resulted in a complete loss of ciliated cells, an increased number of basal cells, and ectopic expressed $Tp63^{-}Krt5^{+}$ putative cells in conducting airways. We provide evidence that *Prmt5*-deficient airway progenitors failed to differentiate into ciliated cells both *in vitro* and *in vivo*. Moreover, the ciliated cell-deficient phenotype was partially rescued by simultaneous downregulation of *Tp63*, which is a direct target of Prmt5. Our results, thus, revealed a novel mechanism in which Prmt5-mediated H4R3sme2 transcriptional repression of Tp63 promotes ciliated cell specification during normal lung development and provides a new potential strategy for targeted therapy of ciliated dysfunction respiratory diseases.

Results

Inactivation of Prmt5 *in the lung epithelium leads to tracheal maldevelopment*

To characterize the physiological functions of Prmt5, we generated a $Prmt5^{fl/fl};Shh^{Cre/+}$ mouse line in which the *Prmt5* was conditionally inactivated in the lung epithelium (24). Prmt5 and its catalytic H4R3sme2 were specifically absent in the airway epithelium of $Prmt5^{fl/fl};Shh^{Cre/+}$ mice as analyzed by Western blotting (Fig. S1, *A* and *B*) and immunofluorescence staining (Fig. S1*C*), whereas the expression of Prmt5 and H4R3sme2 were unaltered in Cdh1-negative mesenchymal cells (Fig. S1*C*). The expression of two other Prmt family proteins (Prmt1 and Prmt7) and H4R3me2 was also unchanged (Fig. S1, *A*–*C*). Alcian blue staining showed a disorganized C-ring tracheal structure of the cartilage in $Prmt5^{fl/fl};Shh^{Cre/+}$ mice at embryonic day 18.5 (E18.5). (Fig. 1*A*), and the trachea of $Prmt5^{fl/fl};Shh^{Cre/+}$ is significantly thinner than controls (Fig. 1*B*). Co-immunostaining of E14.5 tracheas by proximal airway epithelial progenitor marker Sox2 and cartilage progenitor marker Sox9 showed a decreased number of $Sox9^{+}$ cell population in *Prmt5*-deficient mice (9.9 ± 0.38 in control *versus* 2.7 ± 0.21 in *Prmt5* mutant), while the Sox2 expression seems not altered (Fig. 1*C*). H&E staining results revealed that tracheal epithelium was more flattened, and the thickness of the epithelium was significantly reduced in *Prmt5*-deficient mice compared to their littermate controls (Fig. 1, *D* and *E*). Alcian blue and periodic acid–Schiff (AB-PAS) staining analysis showed that there was barely any detectable AB-PAS-positive signaling in the trachea of $Prmt5^{fl/fl};Shh^{Cre/+}$ mice at E18.5 (Fig. 1*F*), implying defects of polysaccharide and protein deposition in *Prmt5*-deficient tracheal epithelium. Further analysis by immunofluorescence staining showed that *Prmt5*-deficient tracheal epithelial cells containing a comparable proportion of Sox2, SSEA1 (a secretory cell-specific marker), and Cdh1 (an epithelial cell membrane-specific expressed adhesion protein) positive cells as controls, although Cdh1 expression seems disorganized (Fig. 1, *G* and *H*). Thus, these results suggest that Prmt5 is required for the normal development of airway epithelium and cartilage.

Failure of ciliated cell specification in the trachea of $Prmt5^{fl/fl};Shh^{Cre/+}$ *mice*

We further performed scanning electron microscopy (SEM) to visualize tracheal epithelium at E18.5. In control mice, the trachea epithelium was composed of cubical secretory cells and cilia-contained ciliated cells. However, no cilia-contained cells were observed, and the cubical cells seem more flatted and bigger in the trachea of $Prmt5^{fl/fl};Shh^{Cre/+}$ mice (Fig. 2*A*). Transmission electron microscope (TEM) analysis also showed that the cilia, as well as the basal body consisting of centrioles at the root of cilia, were absent in the airway epithelium of *Prmt5*-deficient mice (Fig. S2). In line with the SEM and TEM observation results, the absence of cilia structure in $Prmt5^{fl/fl};Shh^{Cre/+}$ tracheal epithelium was further confirmed by immunofluorescence staining using an ac-tubulin antibody, which was reported to be specifically expressed in cilia of mature ciliated cells (30) (Fig. 2*B*). Given that the ciliated cell differentiation is an ordered process that involves initial cell fate determination and subsequential ciliogenesis, we then examined whether airway progenitors could initiate ciliated cell fate specification in *Prmt5*-deficient mice. In control tracheas at E13.5, we observed approximately 11.3% $Sox2^{+}$ epithelial progenitors starting to express Myb (a transcriptional factor whose expression is required for ciliated cell fate specification) (Fig. 2*C*), and approximately 10.8% $Foxj1^{+}$ $Sox2^{+}$ cells appeared at the later developmental stage of E15.5 (Fig. 2*D*). However, neither Myb^{+} nor $Foxj1^{+}$ cells were detected in the trachea of $Prmt5^{fl/fl};Shh^{Cre/+}$ mice at E13.5 and E15.5 (Fig. 2, *C* and *D*). Consistently, RNA-seq analysis revealed that the gene clusters in regulating ciliated cell differentiation were significantly downregulated in the trachea of E13.5 $Prmt5^{fl/fl};Shh^{Cre/+}$ mice (Fig. S3*A*). Notably, the multiciliate differentiation and DNA synthesis–associated cell cycle gene (*Mcidas*) and geminin coiled-coil domain containing (*Gmnc*) gene, that were reported to be essential for initiating ciliated cell lineage differentiation (31), were significantly decreased expressed in $Prmt5^{fl/fl};Shh^{Cre/+}$ tracheas (Fig. S3*A*), which were further confirmed by quantitative real-time-PCR (qRT-PCR) (Fig. S3*B*). Transcription factors, such as Ascl1 (a key factor in initiating neuroendocrine cell differentiation (32)) and Sox2 (essential for maintenance and differentiation of tracheal epithelium (15)), were also downregulated in *Prmt5*-deficient tracheas. Taken together, these experiments suggest that Prmt5 is required for the normal program of ciliated cell specification in airways.

Knockout of Prmt5 *results in aberrant proliferation and differentiation of tracheal epithelial progenitors*

To better characterize the function of Prmt5 during ciliated cell specification, we isolated tracheal progenitors and cultured them in two *in vitro* systems, tracheosphere and air-liquid interface (ALI) culture (33). For tracheosphere culture,

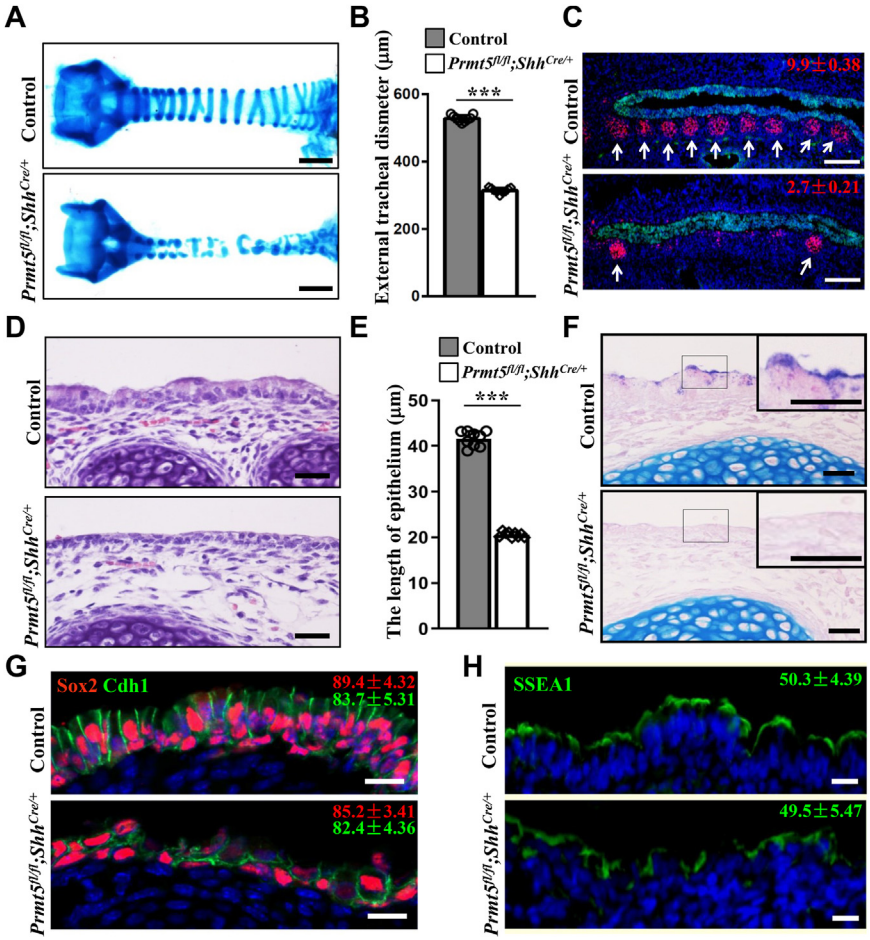

Figure 1. Inactivation of *Prmt5* in the lung epithelium leads to tracheal maldevelopment. *A*, whole-mount alcian blue staining of the trachea at E18.5. The scale bars represent 0.5 mm. *B*, quantification of the external tracheal diameter at E18.5. Quantification was carried out in n = 9 mice per genotype. Each *dot* represents an average of ten points per mouse. *C*, representative trachea sections were co-stained with Sox2 (*green*) and Sox9 (*red*) at E14.5. The scale bars represent 200 μm. *Arrows* indicate Sox9$^+$ cartilage progenitors. The numbers represent the Sox9$^+$ cell populations calculated from ten tracheas. $p < 0.001$. *D*, representative images of H&E-stained E18.5 tracheal sections. *Boxed* areas are magnified in insets. Scale bars represent 50 μm. *E*, quantification of the length of epithelial cells at E18.5. n = 9 mice per genotype. Each *dot* represents an average of ten points per mouse. *F*, representative images of AB-PAS-stained E18.5 tracheal sections. *Boxed* areas are magnified in insets. Scale bars represent 50 μm. *G* and *H*, representative immunofluorescence staining images of E18.5 tracheal sections co-stained by Sox2 (*red*), Cdh1 (*green*) (*E*), and SSEA1(*G*) antibodies. The numbers show the percentage of Sox2$^+$ (*E*) and SSEA1$^+$ (*G*) epithelial cells. $p > 0.05$. The scale bars represent 20 μm. AB-PAS, Alcian blue and periodic acid–Schiff; E, embryonic day; SSEA, stage-specific embryonic antigen.

epithelial progenitors isolated from E13.5 tracheas were cultured in 3D-submerged condition for consecutively 18 days (Fig. 3*A*). Culture of tracheal progenitors from an *mTmG* reporter mouse (*Shh*$^{Cre/+}$;*mTmG*, in which the epithelium was labeled by GFP after Cre recombination (24)) revealed that all formed tracheospheres were GFP-positive (Fig. S4), indicating that these tracheospheres were epithelium-derived. Analysis of tracheospheres showed a significant decrease in the colony-forming efficiency of *Prmt5*-deficient progenitors compared with controls (colony-forming efficiency = 16.79 for control and 4.23 for *Prmt5* mutant) (Fig. 3, *B* and *C*). The diameter of the tracheospheres generated by *Prmt5*-deficient progenitors was on an average about 28.5% smaller than that of the control (99.32 μm for control and 71.08 μm for *Prmt5* mutant) (Fig. 3*D*). To analyze the cell composition of individual tracheospheres, immunofluorescence staining was performed to analyze specific epithelial markers, including Sox2, ac-tubulin, Krt5, and Tp63. In comparison to controls, *Prmt5* mutant tracheospheres contained comparable Sox2$^+$ proximal airway epithelial cells, and increased Tp63$^+$ and Krt5$^+$ basal cells, but were completely absent of ac-tubulin$^+$ ciliated cells (Fig. 3*E*). We further investigated the role of Prmt5 on airway progenitor proliferation and specification in two dimensions (2D)-ALI culture system. Tracheal progenitors were first proliferated in a growth factor–containing medium for 4 days, then were transferred to transwells, and cultured in ALI condition to induce cell differentiation (Fig. 3*A*). During the cell proliferation period, the growth rate of *Prmt5* mutant tracheal progenitors was significantly lower than the control group (Fig. 3*F*). After tracheal progenitor cell differentiation, control ALI cultures differentiated into basal (Tp63$^+$), secretory (Scgb1a1$^+$), and ciliated (Foxj1$^+$ or ac-tubulin$^+$) cells, whereas *Prmt5*-deficient progenitor failed to differentiate into ciliated cells (Fig. 3*G*). Consistently, qRT-PCR analysis revealed that *Foxj1* and *Myb* expression was undetectable in *Prmt5* mutant ALI cultures, while the *Scgb1a1* gene was not significantly

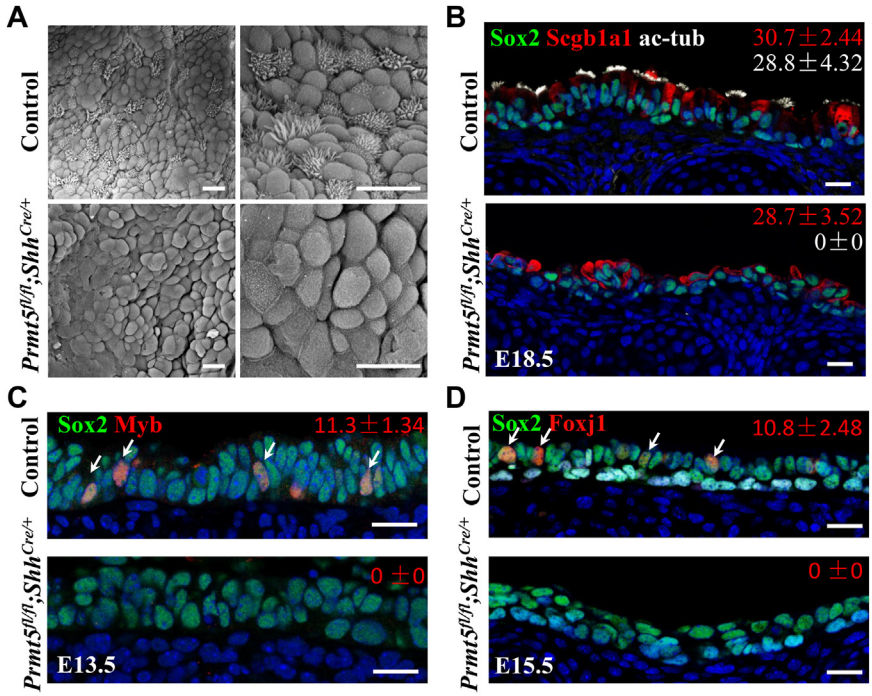

Figure 2. Failure of ciliated cell fate specialization in the trachea of *Prmt5*$^{fl/fl}$;*Shh*$^{Cre/+}$ mice. *A*, representative photomicrographs of scanning electron microscopy (SEM) of trachea cells from control and *Prmt5*$^{fl/fl}$;*Shh*$^{Cre/+}$ mice at E18.5. Magnified pictures were shown on the *right panel*. The scale bars represent 10 μm. *B*, representative triple-immunostaining images of E18.5 tracheal sections by ac-tub (*white*), Scgb1a1 (*red*), and Sox2 (*green*) antibodies. The numbers show the percentage of Scgb1a1$^+$ and ac-tub$^+$ cells. n = 6. $p > 0.05$ for Scgb1a1, $p < 0.001$ for ac-tubulin. The scale bars represent 20 μm. *C* and *D*, representative co-immunostaining images of E13.5 tracheal sections by Myb (*red*) and Sox2 (*green*) antibodies (*C*) and E15.5 tracheal sections by Foxj1 (*red*) and Sox2 (*green*) antibodies (*D*). *Arrows* indicate Myb$^+$ (*C*) and Foxj1$^+$ (*D*) ciliated progenitors in control. The numbers show the percentage of Myb$^+$ and Foxj1$^+$ cells. n = 6. $p < 0.001$. The scale bars represent 20 μm. ac-tub, ac-tubulin, E, embryonic day.

changed (Fig. 3*H*). Collectively, these results suggest that depletion of *Prmt5* in airway progenitors resulted in the compromised proliferation and failed ciliated cell specification.

Elevated Tp63 expression in Prmt5*-deficient tracheal progenitors*

We next attempted to uncover the cell-intrinsic molecular drivers of airway defects after *Prmt5* knockout. RNA-seq results showed that multiple signaling pathways, including ligand–receptor interaction, tight junction, hippo, and Tp53 signaling pathways, were significantly affected by *Prmt5* knockout (Fig. S5*A*). We noticed that two basal cells specifically expressed marker genes (*Tp63* and *Krt5*) were upregulated in *Prmt5*$^{fl/fl}$;*Shh*$^{Cre/+}$ tracheas and significantly increased expression of those genes were also detected by qRT-PCR analysis (Fig. S5*B*), implying an increase in the number of basal cells or elevated expression of these two genes in the individual basal cell. Single-cell RNA sequencing (scRNA-seq) analysis was performed to explore these two possibilities. GFP-positive epithelial cells from the trachea of *Prmt5*$^{fl/+}$;*Shh*$^{Cre/+}$;*mTmG* (control) and *Prmt5*$^{fl/fl}$;*Shh*$^{Cre/+}$;*mTmG* (*Prmt5*$^{fl/fl}$;*Shh*$^{Cre/+}$) mice were manually isolated at E13.5, and then followed by library construction, sequencing, and *t*-distributed stochastic neighbor embedding visualization analysis. Gene ontology analysis of scRNA-seq results indicated that *Prmt5* knockdown significantly affected cell apoptosis, cell division, mRNA splicing, and chromatin modification (Fig. S6*A*), which is in agreement with the well-known functions of Prmt5 (17, 25). Kyoto Encyclopedia of Genes and Genomes analysis revealed that the tight junction and Tp53 pathways, which were altered in bulk RNA-seq analysis, were also significantly changed (Fig. S6*B*). Further analysis of scRNA-seq data revealed that a total of 128 single-cell samples were classified into five clusters based on the overall gene expression similarity (Fig. S7*A*). Clusters 1, 2, and 3 were control-derived cells, while clusters 4 and 5 were almost *Prmt5*$^{fl/fl}$;*Shh*$^{Cre/+}$-derived cells (Fig. S7*B*). Ciliated cell differentiation–related marker genes (*Mcidas*, *Gmnc*, *Foxj1*, and *Myb*) are restricted to be expressed in control clusters. The expression of a known Prmt5 target gene *Cdkn1a* (24), a cell cycle regulator *Ccng1*, and *Tp63* were elevated in the *Prmt5* mutant as expected, while the expression of *Sox2* was decreased in *Prmt5*-deficient cluster 4 cells (Fig. S7*C*). The *Tp63* expression was further analyzed at single-cell resolution, the proportion of Tp63-positive cells, as well as the expression level of Tp63 in individual cells, was significantly higher in the *Prmt5*$^{fl/fl}$;*Shh*$^{Cre/+}$ samples than in the controls (Fig. 4*A*). Consistently, immunofluorescence staining results revealed that although no detectable Tp63-positive signal in control and *Prmt5*$^{fl/fl}$;*Shh*$^{Cre/+}$ tracheas at E12.5, the proportion of Tp63$^+$ cells increased substantially in *Prmt5*$^{fl/fl}$;*Shh*$^{Cre/+}$ tracheal epithelium from the E13.5 onward (Fig. 4, *B–E*). Together, these results indicate that *Prmt5* depletion resulted in high expression of the *Tp63* gene and an increased proportion of Tp63$^+$ cells in airway epithelium.

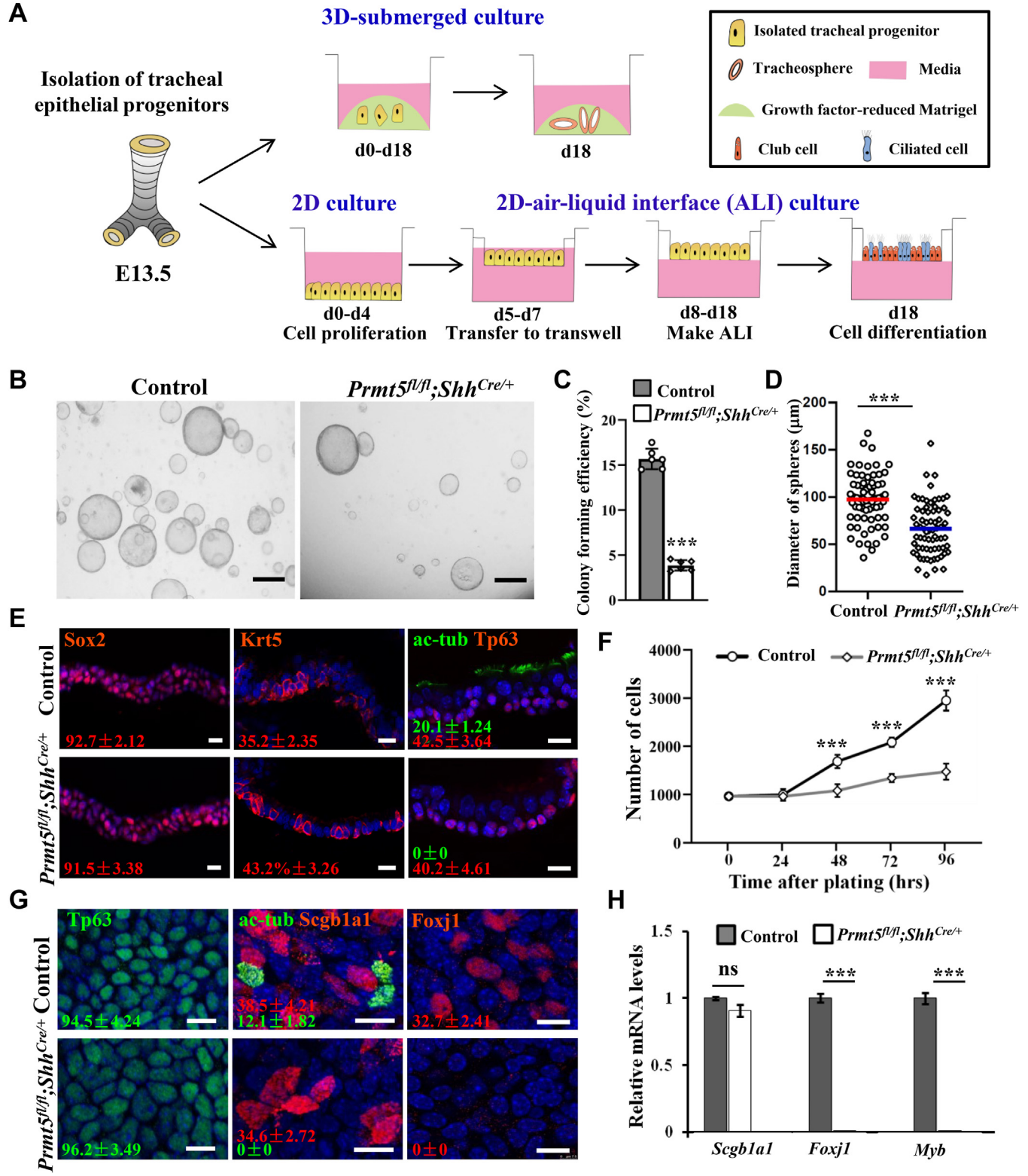

Figure 3. Knockout of *Prmt5* results in abnormal proliferation and differentiation of tracheal epithelial progenitor cells *ex vivo*. *A*, a schematic representation of the assay. Epithelial progenitors were isolated from control and *Prmt5*$^{fl/fl}$;*Shh*$^{Cre/+}$ tracheas at E13.5, and progenitors were subsequently cultured in the 3D condition of 50% Matrigel to grow tracheospheres or 2D condition of air-liquid interface (ALI) culture to induce cell proliferation and differentiation. *B*, representative differential interference contrast images showed a decreased number of tracheospheres in *Prmt5*-deficient cells. The scale bars represent 50 μm. *C* and *D*, statistical analysis of the colonies' formation efficiency (*C*) and the diameter of tracheospheres (*D*). n = 9 wells from 6 pairs of mice. *E*, sections of tracheal *spheres* were stained for Sox2, Krt5, ac-tubulin, and Tp63 antibodies. The numbers show the percentage of each positive cell population, statistics were obtained from 20 tracheospheres. $p < 0.001$ for ac-tubulin, $p > 0.05$ for Sox2, Krt5, and Tp63. The scale bars represent 20 μm. *F*, growth curve of isolated tracheal progenitor cells cultured in 2D conditions is shown; n = 6 pairs. *G*, representative immunostaining images of ALI cultured cells showed defective ciliated cell differentiation of *Prmt5*-deficient tracheal epithelial cells. The numbers show the percentage of Tp63, ac-tubulin, Scgb1a1, and Foxj1-positive cells. $p < 0.001$ for ac-tubulin and Foxj1, $p > 0.05$ for Tp63 and Scgb1a1. The scale bars represent 20 μm. *H*, RT-qPCR analysis of the indicated genes normalized to actin; n = 5 pairs.

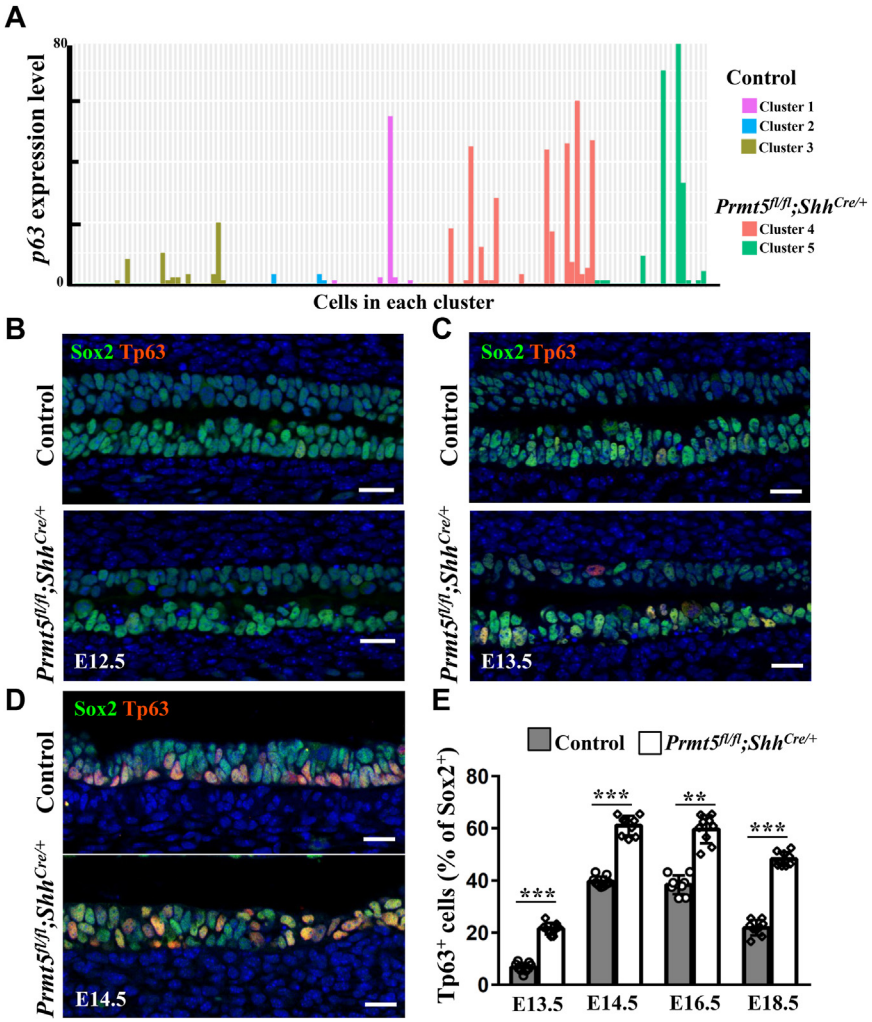

Figure 4. Basal cell-related genes were upregulated in the trachea of *Prmt5*$^{fl/fl}$;*Shh*$^{Cre/+}$ mice. *A*, single-cell RNA sequencing (scRNA-seq) results showing the *Tp63* gene expression pattern in different tracheal epithelial clusters from control and *Prmt5*$^{fl/fl}$;*Shh*$^{Cre/+}$. *B–D*, representative co-immunofluorescence staining images of tracheal sections by Tp63 and Sox2 antibodies at the indicated developmental stages. The scale bars represent 20 μm. *E*, quantification of the number of Tp63$^+$ cells in Sox2$^+$ cells. Quantification was carried out in n = 9 biological replicates from three independent experiments.

Ectopic expressed Tp63$^-$Krt5$^+$ cells in the luminal layer of Prmt5$^{fl/fl}$;Shh$^{Cre/+}$ *trachea*

In the developing airway, progenitors began to differentiate into pseudostratified epithelium structures containing luminal and basal layers, and the Tp63$^+$ progenitors gradually moved toward the basal side and express Krt5 as they differentiate into mature ciliated cells (34). To better characterize Tp63$^+$ epithelial cells, we conducted immunofluorescence co-staining analysis at different developmental stages by using Tp63 and Krt5 antibodies. In control and *Prmt5* mutant tracheas, Tp63$^+$ cells were randomly distributed in the airway epithelium at E14.5, while they localized only on the basal layer and co-expressed Krt5 at E16.5 and E18.5 (Fig. 5, *A–C*). Notably, the number of Tp63$^+$ and Krt5$^+$ cells increased substantially in the *Prmt5* mutant at all detected stages (Fig. 5, *A–C*). Interestingly, in contrast to control, a subpopulation of Tp63$^+$Krt5$^+$ cells was detected in the trachea of *Prmt5* mutant at E14.5, while a subpopulation of Tp63$^-$Krt5$^+$ cells resided in the luminal layer (Fig. 5, *A–C*). Quantitative analysis revealed that the Tp63$^-$Krt5$^+$ cells account for almost 10% of the airway epithelium in *Prmt5*$^{fl/fl}$;*Shh*$^{Cre/+}$ mice at E16.5 and E18.5, whereas these cells were not detected in the controls (Fig. 5*D*). We further characterized whether these Tp63$^-$Krt5$^+$ cells were a subpopulation of secretory cells, immunofluorescence staining analysis showed that the Tp63$^-$Krt5$^+$ cells did not co-express secretory cell-specific marker genes Scgb3a2 and Scgb1a1 (Fig. 5*E*). We defined these Tp63$^-$Krt5$^+$ cells as putative cells, which are specifically expressed in the luminal side of *Prmt5*-deficient airway with undefined lineage and physiological functions.

Prmt5 and H4R3sme2 modulate chromatin configuration at the Tp63 *locus*

One of the epigenetic mechanisms of Prmt5 in biological processes is to regulate gene transcription through methylated histone substrates (17), and Tp63 has been implicated in the inhibition of ciliated cell lineage differentiation (13). As the deficiency of ciliated cells in the *Prmt5* mutant trachea was

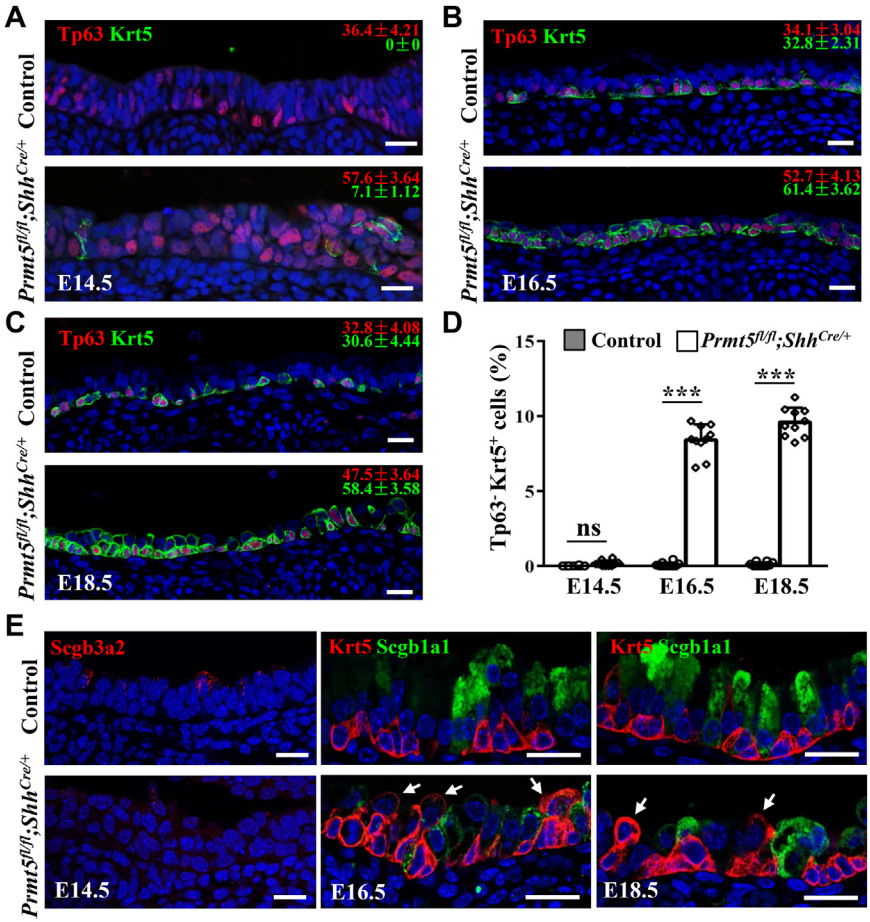

Figure 5. Ectopically expressed Krt5$^+$ cells in the trachea of *Prmt5$^{fl/fl}$;Shh$^{Cre/+}$* mice. *A–C* representative co-immunostaining images of tracheal sections by Tp63 and Krt5 antibodies at the indicated developmental stages. Numbers indicate the percentage of Krt5$^+$ and Tp63$^+$ cells, respectively. The scale bars represent 20 μm. *D*, quantification of Tp63$^-$Krt5$^+$ cells in the trachea of control and *Prmt5$^{fl/fl}$;Shh$^{Cre/+}$* mice. n = 10 pairs. *E*, representative immunofluorescence images of tracheal sections with indicated antibodies. *Arrows* point to the Tp63$^-$Krt5$^+$ cells. The scale bars represent 20 μm.

accompanied by elevated Tp63 expression, we next examined the possibility that Prmt5 represses *Tp63* transcription through histone arginine methylation modifications. Chromatin immunoprecipitation-qPCR (ChIP-qPCR) assay was performed to detect whether Prmt5 and H4R3sme2 (a Prmt5 catalyzed histone modification that globally represses gene expression (35)) proteins binding to chromatin of the ΔN isoform of Tp63 (ΔNTp63, the reported predominant Tp63 isoform in airway epithelium (36)) locus. With multiple primer sets spanning a 2.5 kb region relative to the putative *ΔNTp63* transcriptional start site, we detected binding signals for Prmt5 and H4R3sme2 at sites g and h of the *ΔNTp63* promoter, as well as at C40 enhancer regions in E14.5 tracheas of WT mice (Fig. 6, *A–C*). ChIP signaling was significantly reduced in *Prmt5*-deficient epithelial cells demonstrating the specificity (Fig. 6, *D* and *E*). We then examined an active histone marker H3K4me3 (tri-methylated lysine 4 of histone H3) and a repressive histone mark H3K27me3 (tri-methylated lysine 27 of histone H3), at the *ΔNTp63* locus in control and *Prmt5*-deficient epithelial cells. Consistent with the increased expression of Tp63 in *Prmt5* mutant tracheas, we observed a significantly increased ChIP signaling of H3K4me3 and a significantly decreased ChIP signaling of H3K27me3 in the *ΔNTp63* promoter regions of Prmt5 binding with (Fig. 6, *F* and *G*). These results thus suggest that Prmt5 modulates chromatin configuration at the Tp63 locus through H4R3sme2, thereby repressing its transcription.

Inhibition of Tp63 *in* Prmt5$^{fl/fl}$;Shh$^{Cre/+}$ *tracheal progenitors rescues the ciliated cell-deficient phenotype*

To further specify the role of Prmt5 in promoting ciliated cell differentiation by inhibiting Tp63 expression, tracheal epithelial progenitors were treated with a well-characterized Prmt5 inhibitor EPZ015666, which was reported to selectively inhibit Prmt5 enzymatic activity (37) under ALI culture conditions. EPZ015666 treatment of airway progenitors resulted in elevated *Tp63* expression (Fig. S8*A*) as well as remarkably impaired ciliated cell differentiation (Fig. S8*B*). We next determined whether the elevated Tp63 expression directly contributes to the ciliated cell deficiency phenotype in *Prmt5$^{fl/fl}$;Shh$^{Cre/+}$* mice. The *Tp63* expression was inhibited in tracheal progenitors by lentiviral-mediated two different shRNAs that are complementary to different portions of *Tp63* mRNA, and a nontargeting scrambled shRNA was used as control. Infected progenitors were either cultured on Matrigel

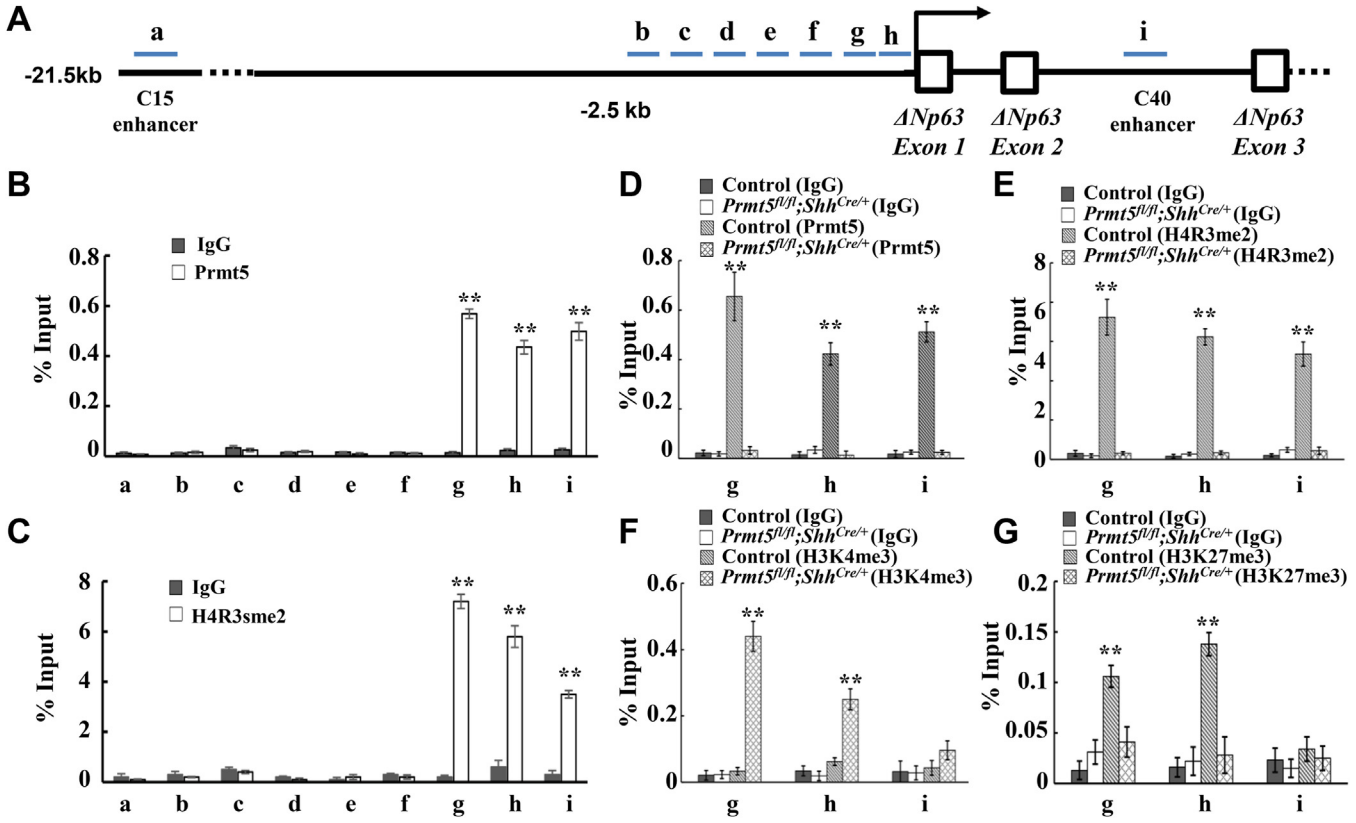

Figure 6. Prmt5 targets *Tp63* to regulate airway epithelial cell differentiation. *A*, schematic diagrams of the mouse *ΔNp63* gene structure. *Blue bars* represent the regions examined by ChIP; *white boxes* represent exons; *black lines* represent introns. *B–G*, ChIP analysis results of *ΔNTp63* gene with Prmt5 (*B* and *D*), H4R3sme2 (*C* and *E*), H3K4me3 (*F*), and H3K4me3 (*G*) antibodies. All fold changes were normalized to input. The data shown are the mean ± S.D of three independent experiments. ChIP, chromatin immunoprecipitation.

to grow tracheospheres or cultured on ALI conditions for the indicated time to allow cell differentiation (Fig. 7*A*). Immunofluorescence staining results showed that the presence of ac-tubulin$^+$ mature ciliated cells after knockdown of *Tp63* in *Prmt5*-deficient airway progenitors, both in tracheospheres cultured for 16 days (Fig. 7*B*) and ALI culture for 18 days (Fig. 7*C*). Quantitative analysis revealed that the proportion of ac-tubulin$^+$ cells in *Prmt5*-mutant were significantly lower compared with that of controls in tracheospheres (Fig. 7*D*) and ALI cultures (Fig. 7*E*). The two *Tp63* shRNAs exhibited roughly equivalent numbers of ciliated cells in the *Prmt5* mutant that did not reach the control levels (Fig. 7, *D* and *E*). Therefore, these findings suggest that Prmt5 *via* H4R3sme2 represses Tp63 transcription in airway epithelial progenitor cells, thereby promoting the specification of ciliated cells, whereas *Prmt5*-deficiency results in the high Tp63 expression that failed to differentiate into ciliated cell lineage (Fig. S8*C*).

Discussion

We have previously reported that lung epithelial-specific inactivation of *Prmt5* led to halted branching morphogenesis and neonatal death (24). In this study, we show that Prmt5 is critical for airway epithelium cell fate specification. The *Prmt5* mutant trachea exhibited increased Tp63$^+$ airway progenitors and mature basal cells, completely absent ciliated cells, as well as ectopically expressed Tp63$^-$Krt5$^+$ putative cells (Fig. 8). Inactivation of *Tp63* in the *Prmt5*-deficient airway epithelial progenitors leads to the reversal of ciliated cell depletion defect. While our previous work describes the importance of Prmt5 in lung morphogenesis, the current study highlights Prmt5 as a crucial player in airway ciliated cell fate specification during lung development.

Our work identified the master basal cell transcription factor ΔNTp63, a homolog of the tumor-suppressor Tp53, as a direct target of Prmt5 during airway epithelial cell fate specification. Tp63, specifically its predominant isoform ΔNTp63, is abundantly expressed in basal stem cells of various proliferative epithelial tissues and plays a key role in the maintenance of basal cell identity, proliferation, and differentiation (38–42). The role of Tp63 in airway epithelial cell specification is controversial. Complete deletion of *Tp63* leads to abnormally increased ciliated cells in the airway epithelium (13). Consistently, Marshall *et al.*(43) reported that Tp73 and Tp63 are co-expressed in ciliated cells, and are required for ciliated cell differentiation. In contrast, although significantly increased ac-tubulin$^+$ and decreased SSEA1$^+$ cells were detected in the trachea epithelium of tamoxifen-induced *Tp63* KO mouse, the distribution of secretory and ciliated cells was comparable between control and *Tp63* KO mouse (44). We speculate that the disparity in these results could be due to the different *Tp63*-KO time points and efficiency in different genetically

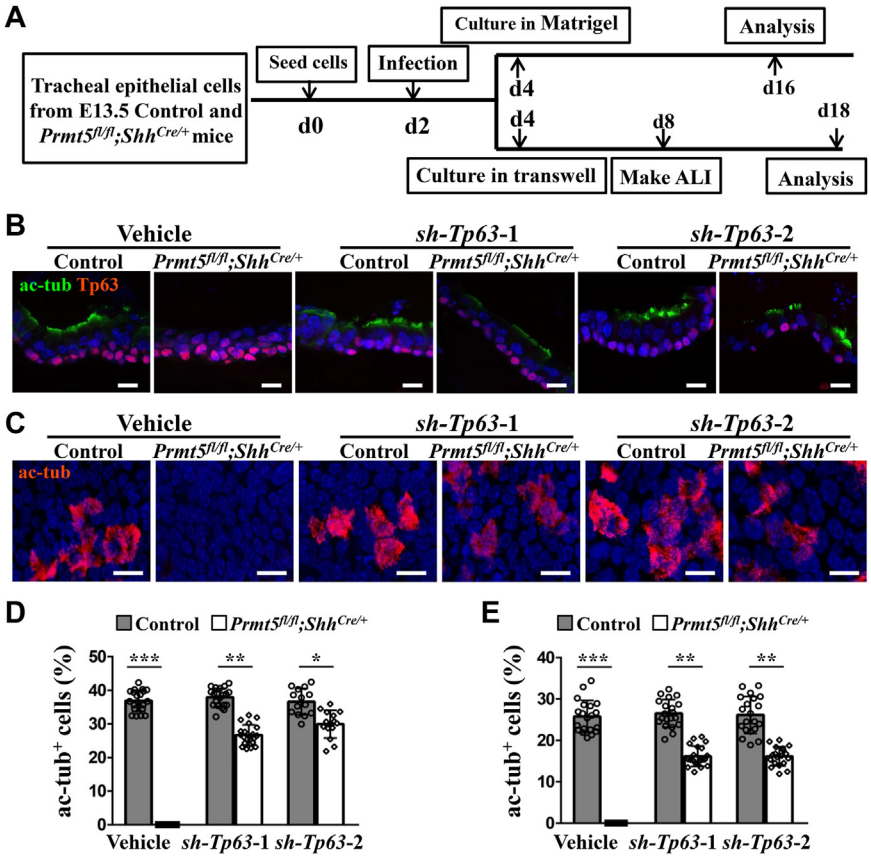

Figure 7. Inhibition of *Tp63* partially restores the ciliated cell specification defects in *Prmt5*-deficient tracheal epithelial cells. *A*, schematic representation of infection and culture of mouse tracheal epithelial progenitors. On day 2, cells were infected with either vector or *sh-Tp63*, and infected cells were transferred to 50% Matrigel or ALI culture on day 4, and analyzed at the indicated time point. *B* and *C* representative co-immunofluorescence staining images of tracheospheres (*B*) and ALI cultures (*C*). The scale bars represent 20 μm. *D* and *E*, quantification of the percentage of ac-tubulin$^+$ cells from tracheospheres (*B*) and ALI cultures (*C*). n > 6 animals per genotype. ALI, air-liquid interface.

modified mice models. Alternatively, it could be due to other unidentified Tp63 cofactors involved in airway epithelial cell fate determination. In this work, as the ciliated cells loss phenotype was partially restored by knockdown of *Tp63* in *Prmt5*-deficient tracheal progenitors, our results suggest that the Tp63 is transcriptionally repressed by Prmt5 mediated H4R3sme2, and it is functionally required for ciliated cell specification.

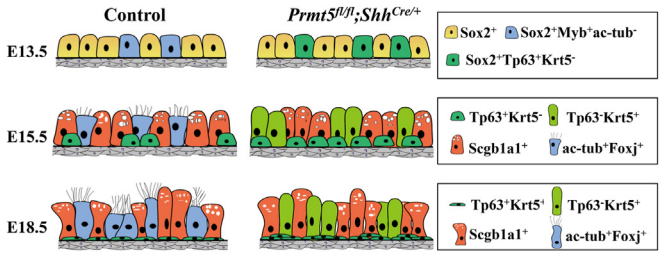

Figure 8. Working model of Prmt5 during tracheal epithelial cell fate specification. During normal lung development (control), a subpopulation of airway progenitors (*blue*) started to commit ciliated cell fate specification at E13.5, cell fate was committed to basal (*green*), secretary (*orange-red*), or ciliated (*blue*) cells at E15.5, and further differentiated into mature basal, secretory, and ciliated cells at E18.5. In the trachea of *Prmt5*$^{fl/fl}$;*Shh*$^{Cre/+}$ mice, progenitors failed to commit ciliated cell specification, and a few populations (*green*) start to express basal cell maker gene Tp63 at E13.5, resulting in an increased number of premature/mature basal cells, absence of ciliated cells, and a population of Tp63$^-$Krt5$^+$ putative cells at E15.5 and E18.5. E, embryonic day.

The appearance of Tp63$^-$Krt5$^+$ cells in the airway of *Prmt5*$^{fl/fl}$;*Shh*$^{Cre/+}$ mice is intriguing. A subpopulation of Tp63$^+$Krt5$^+$ cells was first detected at E14.5, and the Tp63$^-$Krt5$^+$ putative cells were detected at later developmental stages (E16.5 and E18.5), indicating that these putative cells are probably derived from Tp63$^+$Krt5$^+$ cells. Previous work has revealed that Tp63$^+$ basal progenitors in the trachea arise around E13.5, these cells start to migrate to the basal side of the pseudostratified airway epithelium and express the other basal cell marker Krt5 (6, 44). Mature basal cells are stem cells of the mouse trachea and human airway epithelium, capable of self-renewal and differentiation into both secretory and ciliated epithelial lineages (45, 46). In the intrapulmonary airways, a rare Tp63$^+$/Krt5$^-$ basal cell derivative population responds to the H1N1, COVID-19 virus, and bleomycin-induced severe lung injury (47–49). A recent study identified six subpopulations in the adult murine trachea using a scRNA-seq approach, suggesting a high degree of heterogeneity of the basal cell (50). The Tp63$^-$Krt5$^+$ cells expressed in the luminal layer of the *Prmt5* mutant could be intermediate state cells driven from Tp63$^+$ basal cells differentiated into ciliated or other luminal cell fate or might be a new cell type formed under specified conditions. Additionally, this Tp63$^-$Krt5$^+$ cell population was also observed in the luminal side of *Fbxw7* mutant tracheas previously (11). Inactivation of Notch1 in the

Fbxw7 mutant background reversed ectopic Tp63^{-}Krt5^{+} cell phenotype (11), suggesting that Notch1 is critical for Tp63^{-}Krt5^{+} cell specification. It remains undetermined whether the same cell type appears in the *Fbxw7* and *Prmt5* mutants. Animal models containing Tp63^{-}Krt5^{+} cells provide key experimental materials for studying airway epithelial cell fate determination and epithelium heterogeneity.

In summary, our findings underscore a key role for Prmt5 and H4R3sme2 in promoting the specific differentiation of respiratory epithelial progenitors to ciliated cells. Given the association of aberrant ciliated cell differentiation with multiple human respiratory diseases, our study lays the ground for future investigation of the functional contribution and potential molecular mechanisms of Prmt5 to the pathogenesis of ciliated cell-related diseases.

Experimental procedures

Animals

All animal works were performed following the guidelines set by the animal welfare committees of Anhui University. The lung epithelium-specific *Prmt5* KO mice ($Prmt5^{fl/fl};Shh^{Cre/+}$) were produced by crossing $Prmt5^{fl/+};Shh^{Cre/+}$ mice with $Prmt5^{fl/fl}$ mice as previously described (24). Rosa26-mTmG reporter mice were kindly gifted by Prof John Speakman from the Institute of Genetics and Developmental Biology-Chinese Academy of Sciences. $Prmt5^{fl/+};Shh^{Cre/+};mTmG$ and $Prmt5^{fl/fl};Shh^{Cre/+};mTmG$ mice used for sc-RNA-seq were generated by crossing mTmG males with $Prmt5^{fl/fl}$ females. The embryos used in this study were harvested from time-mated females, and at noon of the day when a vaginal plug was detected was considered as E0.5. All mice used in this study were bred in congenic C57BL/6 background and genotyped by genomic DNA PCR using primers listed in Table S1.

Sectional AB-PAS staining and H&E staining

Sectional AB-PAS and H&E staining were performed as described previously (51). Briefly, tracheas isolated from E18.5 control and $Prmt5^{fl/fl};Shh^{Cre/+}$ mice were fixed in 4% paraformaldehyde (PFA, Sigma-Aldrich, P6148) overnight at 4 °C, then processed to paraffin (Thermo Fisher Scientific, 8330) embedding and sectioned at 5 μm thickness. The deparaffinized and rehydrated tracheal sections were stained with an AB-PAS staining kit (Solarbio, G1285) or H&E staining kit (Leagene, DH0006), respectively, according to the manufacturer's instructions.

Whole-mount alcian blue staining

E18.5 tracheas from control or $Prmt5^{fl/fl};Shh^{Cre/+}$ mice were first fixed with 4% PFA, washed extensively with PBS, then immersed in a mixture of 95% ethanol (80 ml) and acetic acid (20 ml) containing 10 mg alcian blue 8GX (Sigma-Aldrich, 05500), and maintained at room temperature overnight. Tracheas were finally cleared in 1% KOH (Sigma-Aldrich, 484016) solution until the C-ring cartilage was visible.

SEM and TEM assay

For SEM assay, E18.5 tracheal samples were fixed in 5% in 4% PFA at 4 °C overnight and dehydrated in a series of graded ethanol. The ventral side of the tracheas was then analyzed without a conductive coating by using a Zeiss EVO 15 SEM (Carl Zeiss Microscopy GmbH). TEM assay was performed as previously reported (51). Briefly, isolated tracheas were fixed in 2.5% glutaraldehyde and then in 1% OsO4 on ice for 2 h, dehydrated in graded acetone solutions and embedded in EMbed 812 resin (Electron Microscopy Sciences, 13940). Ultrathin sections (65 nm) were stained with 2% uranyl acetate for 30 min and lead citrate for 10 min. Images were acquired using a 120 kV electron microscope (JEM America Corp).

Immunofluorescence staining and imaging

Immunofluorescence staining was performed following a previously published protocol (24). Briefly, frozen sections (8-μm-thickness) were pretreated with 0.5% Triton X-100 (Sigma-Aldrich, T8787) in PBS for 15 min. After blocking, sections were incubated with primary antibodies overnight at 4 °C followed by 2 h of incubation with appropriate secondary antibodies and counterstained with DAPI (Sigma-Aldrich, D9542). Images were acquired using a Leica TCS SP8 DIVE confocal microscope. The antibodies used are listed in Table S2.

Tracheosphere culture

Mouse tracheosphere culture was performed as previously described (52). Tracheal epithelial progenitors were suspended in mouse tracheal epithelial cells (MTEC)-plus medium (Table S3), mixed at a 1:1 ratio with growth factor-reduced Matrigel (BD, 354230), and seeded at 800 cells per well in 24-well plates (Corning, 353047) coated with 20 μl of 100% Matrigel. The medium was changed every other day. Images were taken on day 18 using an Axiovert 200 M microscope (Carl Zeiss). For statistical analysis, the number of tracheospheres per insert was counted. Samples were set up in triplicates from at least six biological replicates. For immunofluorescence staining analysis, tracheospheres were fixed with 4% PFA for 30 min, immersed in 10% sucrose (Sigma-Aldrich, V900116) in PBS overnight at 4 °C, followed by embedding in optimal cutting temperature compound (Sakura, 4853) and sliced to 8 μm.

ALI culture

Isolated tracheal epithelial progenitors were cultured on rat tail collagen type I (Sigma-Aldrich, C7661)-coated plastics, grown for 4 days in MTEC-plus medium to reach confluent. Cells were then trypsinized and seeded at 1000 cells per well in a 24-well, 0.4-μm pore size membrane transwell insert (Corning, 3413). The MTEC-plus medium was added to both the apical and inferior chambers and changed every other day. The apical medium was removed on day eight to induce cell differentiation. Cells were fixed for immunofluorescence staining or collected for qRT-PCR analysis on day 18. For the EPZ015666 treatment, 10 μm of EPZ015666

(MedChemExpress, HY-12727) was continuously supplied throughout the ALI culture. For quantification, α-tubulin$^+$ or Foxj1$^+$ cells were counted in randomly selected areas, except for the area within 1 mm from the edge of the transwell insert.

Knockdown of Tp63 *in tracheal progenitors*

To knockdown *Tp63* in tracheal progenitors, lentivirus containing a U6 promoter to express *Tp63* shRNA (Gene ID: NM-011641.2; Target sequence: GGAATGAACAGACG TCCAA for *Tp63–1* and GCTGAGCCGTGAGTTCAAT for *Tp63–2*) were ordered at Obio Technology Co, Ltd, and a nontargeting scrambled shRNA construct was used as negative control. Tracheal progenitors were seeded onto collagen I-coated 24-well plates (STEMCELL Technologies, 100-0364) and grown for 48 h. The cells were transduced with 20 μl lentiviral particles in a 500 μl MTEC-plus medium. After 48 h of infection, cells were trypsinized and transferred to 50% Matrigel for tracheosphere culture or transwell inserts for ALI culture as indicated.

scRNA-seq analysis

Tracheas from *Prmt5$^{flox/+}$;Shh-Cre;mTmG* (control) and *Prmt5$^{flox/flox}$;Shh-Cre;mTmG* (*Prmt5$^{fl/fl}$;Shh$^{Cre/+}$*) mice were minced with sterilized scissors after washing three times with PBS, and then digested in 1 mg/ml collagenase type IV (Gibco, 17104019) at 37 °C for 15 min. The digestion process was stopped by adding Dulbecco's modification of Eagle's medium containing 10% fetal bovine serum (Gibco, 10099141C). GFP$^+$ single cells were picked up under a stereomicroscope using the single-cell pipette sampling platform of the Beijing Institute of Genomics, Chinese Academy of Sciences. The scRNA-seq library was prepared using the single-cell tagged reverse transcription sequencing protocol (53), and sequencing was performed on the Illumina HiSeq X TEN platform. Data analyses were proceeded as previously described (54).

Bulk RNA-sequencing

RNA-sequencing was conducted as previously described (24). In brief, total RNA was extracted from the E13.5 trachea of control and *Prmt5$^{fl/fl}$;Shh$^{Cre/+}$* mice. The sequencing was performed on an Illumina HiSeq X TEN platform and libraries were generated using a NEBNext Ultra II RNA Library Prep Kit for Illumina (NEB, E7770). The DESeq R package (1.18.0) was used for differential expression analysis. Datasets are deposited in the Gene Expression Omnibus database under accession number GSE229423.

RNA extraction and qRT-PCR

Total RNA was prepared using TRIzol reagent (Ambion, 15596-026). The first strand complementary DNA was reverse transcribed with a FastQuant RT Kit (TIANGEN, kr106-02. qRT-PCR analysis was performed on an Agilent Technologies Strata Gene Mx3000P system using SYBR Green (Vazyme, Q511-02). Gene expression levels were normalized to internal β-actin. The primers were listed in Table S1.

ChIP assay

ChIP was performed according to the protocol described previously (55), using E14.5 WT tracheas or isolated airway epithelial cells. The primers for qPCR detection of *Tp63* chromatin regions were provided in Table S1.

Quantification and statistical analysis

All quantification data were collected from at least three independent experimental replications. And the exact number of replicates (n) for each experiment was described in the relevant figure legends. Data were presented as means ± S.D. *p*-values were calculated with GraphPad Prism, version 8 (GraphPad Software, www.graphpad.com). We used a two-tailed unpaired Student's *t* test for comparison between two experimental groups and one-way ANOVA for multiple comparisons. Before making comparisons, the normality of distributions was tested and the variance was similar between groups. All statistics represent biological replicates. ns, not significant, $^*p < 0.05$, $^{**}p < 0.01$, $^{***}p < 0.001$.

Ethics statement

This study was performed by the principles of the Helsinki Declaration of the World Medical Association. All animal work was carried out in accordance with the protocols approved by the animal welfare committee of Anhui University (IACUC(AHU)-2022-012).

Data availability

All data analyzed during this study are included in this published article and its supplementary files. The detailed experimental procedures and the materials will be freely available to the scientific community upon reasonable request.

Supporting information—This article contains supporting information.

Acknowledgments—We thank Prof Lin Xinhua (Fudan University) for his kind gift of the *Shh$^{cre/+}$* mice. We also thank the staff of the facility of the Institute of Health Sciences & Technology, Anhui University, for providing technical support. This work was supported by grants from the National Natural Sciences Foundation of China (32270880, 32170834), the Natural Sciences Foundation of Anhui Province of China (2018085MC82), and the National Key R&D Program of China (2022YFC3600202, 2018YFA0800902).

Author contributions—Q. Li and S. B. conceptualization; Q. Li and S. B. project administration; Q. Li and S. B. writing–original draft; Q. Li, J. J., and H. L. methodology; J, J., Y. H., Q. Lu, Y. Z., and H. L. investigation; Q. Li, J. J., Y. H., Q. Lu, Y. Z., and H. L. formal analysis; J. C., M. M., and S. B. writing–review and editing.

Conflict of interest—The authors declare that they have no conflicts of interest with the contents of this article.

Abbreviations—The abbreviations used are: ALI, air-liquid interface; AB-PAS, Alcian blue and periodic acid–Schiff; ChIP-qPCR, chromatin immunoprecipitation-qPCR; E, embryonic day; Krt5, keratin

5; MTEC, mouse tracheal epithelial cells; PFA, paraformaldehyde; Prmt5, protein arginine methyltransferase 5; qRT-PCR, quantitative real-time-PCR; scRNA-seq, single-cell RNA sequencing; SEM, scanning electron microscopy; TEM, transmission electron microscope; Tp63, transformation-related protein 63.

References

1. Zepp, J. A., and Morrisey, E. E. (2019) Cellular crosstalk in the development and regeneration of the respiratory system. *Nat. Rev. Mol. Cell Biol.* **20**, 551–566
2. Barrios, J., Kho, A. T., Aven, L., Mitchel, J. A., Park, J. A., Randell, S. H., *et al.* (2019) Pulmonary Neuroendocrine Cells Secrete γ-Aminobutyric acid to induce goblet cell hyperplasia in primate models. *Am. J. Respir. Cell Mol. Biol* **60**, 687–694
3. Montoro, D. T., Haber, A. L., Biton, M., Vinarsky, V., Lin, B., Birket, S. E., *et al.* (2018) A revised airway epithelial hierarchy includes CFTR-expressing ionocytes. *Nature* **560**, 319–324
4. Plasschaert, L. W., Žilionis, R., Choo-Wing, R., Savova, V., Knehr, J., Roma, G., *et al.* (2018) A single-cell atlas of the airway epithelium reveals the CFTR-rich pulmonary ionocyte. *Nature* **560**, 377–381
5. Rock, J. R., Gao, X., Xue, Y., Randell, S. H., Kong, Y. Y., and Hogan. (2011) Notch-dependent differentiation of adult airway basal stem cells. *Cell Stem Cell* **8**, 639–648
6. Basil, M. C., Katzen, J., Engler, A. E., Guo, M., Herriges, M. J., Kathiriya, J. J., *et al.* (2020) The cellular and physiological basis for lung repair and regeneration: past, present, and future. *Cell Stem Cell* **26**, 482–502
7. Tan, F. E., Vladar, E. K., Ma, L., Fuentealba, L. C., Hoh, R., Espinoza, F. H., *et al.* (2013) Myb promotes centriole amplification and later steps of the multiciliogenesis program. *Development* **140**, 4277–4286
8. Morimoto, M., Liu, Z., Cheng, H. T., Winters, N., Bader, D., and Kopan, R. (2010) Canonical Notch signaling in the developing lung is required for determination of arterial smooth muscle cells and selection of Clara versus ciliated cell fate. *J. Cell Sci.* **123**, 213–224
9. Morimoto, M., Nishinakamura, R., Saga, Y., and Kopan, R. (2012) Different assemblies of Notch receptors coordinate the distribution of the major bronchial Clara, ciliated and neuroendocrine cells. *Development* **139**, 4365–4373
10. Chu, Q., Yao, C., Qi, X., Stripp, B. R., and Tang, N. (2019) STK11 is required for the normal program of ciliated cell differentiation in airways. *Cell Discov.* **5**, 36
11. Li, R., Zhang, Y., Garg, A., Sui, P., and Sun, X. (2022) E3 ubiquitin ligase FBXW7 balances airway cell fates. *Dev. Biol.* **483**, 89–97
12. Eenjes, E., Buscop-van Kempen, M., Boerema-de Munck, A., Edel, G. G., Benthem, F., de Kreij-de Bruin, L., *et al.* (2021) SOX21 modulates SOX2-initiated differentiation of epithelial cells in the extrapulmonary airways. *Elife* **10**, e57325
13. Daniely, Y., Liao, G., Dixon, D., Linnoila, R. I., Lori, A., Randell, S. H., *et al.* (2004) Critical role of p63 in the development of a normal esophageal and tracheobronchial epithelium. *Am. J. Physiol. Cell Physiol.* **287**, C171–C181
14. Tompkins, D. H., Besnard, V., Lange, A. W., Wert, S. E., Keiser, A. R., Smith, A. N., *et al.* (2009) Sox2 is required for maintenance and differentiation of bronchiolar Clara, ciliated, and goblet cells. *PLoS One* **4**, e8248
15. Que, J., Luo, X., Schwartz, R. J., and Hogan, B. L. (2009) Multiple roles for Sox2 in the developing and adult mouse trachea. *Development* **136**, 1899–1907
16. Chen, J., Knowles, H. J., Hebert, J. L., and Hackett, B. P. (1998) Mutation of the mouse hepatocyte nuclear factor/forkhead homologue 4 gene results in an absence of cilia and random left-right asymmetry. *J. Clin. Invest.* **102**, 1077–1082
17. Stopa, N., Krebs, J. E., and Shechter, D. (2015) The PRMT5 arginine methyltransferase: many roles in development, cancer and beyond. *Cell. Mol. Life Sci.* **72**, 2041–2059
18. Maron, M. I., Casill, A. D., Gupta, V., Roth, J. S., Sidoli, S., Query, C. C., *et al.* (2022) Type I and II PRMTs inversely regulate post-transcriptional intron detention through Sm and CHTOP methylation. *Elife* **11**, e72867
19. K. M. Mulvaney, Blomquist, C., Acharya, N., Li, R., Ranaghan, M. J., O'Keefe, M., et al., Molecular basis for substrate recruitment to the PRMT5 methylosome. *Mol. Cell* **81**, (2021), 3481–3495.e3487
20. Wu, Q., Schapira, M., Arrowsmith, C. H., and Barsyte-Lovejoy, D. (2021) Protein arginine methylation: from enigmatic functions to therapeutic targeting. *Nat. Rev. Drug Discov.* **20**, 509–530
21. Bezzi, M., Teo, S. X., Muller, J., Mok, W. C., Sahu, S. K., Vardy, L. A., *et al.* (2013) Regulation of constitutive and alternative splicing by PRMT5 reveals a role for Mdm4 pre-mRNA in sensing defects in the spliceosomal machinery. *Genes Dev.* **27**, 1903–1916
22. Wang, J., Huang, X., Zheng, D., Li, Q., Mei, M., and Bao, S. (2022) PRMT5 determines the pattern of polyploidization and prevents liver from cirrhosis and carcinogenesis. *J. Genet. Genomics* **50**, 87–98
23. Tee, W. W., Pardo, M., Theunissen, T. W., Yu, L., Choudhary, J. S., Hajkova, P., *et al.* (2010) Prmt5 is essential for early mouse development and acts in the cytoplasm to maintain ES cell pluripotency. *Genes Dev.* **24**, 2772–2777
24. Li, Q., Jiao, J., Li, H., Wan, H., Zheng, C., Cai, J., *et al.* (2018) Histone arginine methylation by Prmt5 is required for lung branching morphogenesis through repression of BMP signaling. *J. Cell Sci.* **131**, jcs217406
25. Tan, D. Q., Li, Y., Yang, C., Li, J., Tan, S. H., Chin, D. W. L., *et al.* (2019) PRMT5 modulates splicing for genome integrity and preserves proteostasis of hematopoietic stem cells. *Cell Rep* **26**, 2316–2328.e2316
26. Zhang, T., Günther, S., Looso, M., Künne, C., Krüger, M., Kim, J., *et al.* (2015) Prmt5 is a regulator of muscle stem cell expansion in adult mice. *Nat. Commun.* **6**, 7140
27. Banasavadi-Siddegowda, Y. K., Russell, L., Frair, E., Karkhanis, V. A., Relation, T., Yoo, J. Y., *et al.* (2017) PRMT5-PTEN molecular pathway regulates senescence and self-renewal of primary glioblastoma neurosphere cells. *Oncogene* **36**, 263–274
28. Dong, F., Chen, M., Chen, M., Jiang, L., Shen, Z., Ma, L., *et al.* (2021) PRMT5 is involved in spermatogonial stem cells maintenance by regulating Plzf expression via modulation of lysine histone modifications. *Front. Cell Dev. Biol.* **9**, 673258
29. Li, Z., Yu, J., Hosohama, L., Nee, K., Gkountela, S., Chaudhari, S., *et al.* (2015) The Sm protein methyltransferase PRMT5 is not required for primordial germ cell specification in mice. *EMBO J* **34**, 748–758
30. Clare, D. K., Magescas, J., Piolot, T., Dumoux, M., Vesque, C., Pichard, E., *et al.* (2014) Basal foot MTOC organizes pillar MTs required for coordination of beating cilia. *Nat. Commun.* **5**, 4888
31. Treutlein, B., Brownfield, D. G., Wu, A. R., Neff, N. F., Mantalas, G. L., Espinoza, F. H., *et al.* (2014) Reconstructing lineage hierarchies of the distal lung epithelium using single-cell RNA-seq. *Nature* **509**, 371–375
32. Sui, P., Wiesner, D. L., Xu, J., Zhang, Y., Lee, J., Van Dyken, S., *et al.* (2018) Pulmonary neuroendocrine cells amplify allergic asthma responses. *Science* **360**, eaan8546
33. Liberti, D. C., and Morrisey, E. E. (2021) Organoid models: assessing lung cell fate decisions and disease responses. *Trends Mol. Med.* **27**, 1159–1174
34. Hogan, B. L., Barkauskas, C. E., Chapman, H. A., Epstein, J. A., Jain, R., Hsia, C. C., *et al.* (2014) Repair and regeneration of the respiratory system: complexity, plasticity, and mechanisms of lung stem cell function. *Cell Stem Cell* **15**, 123–138
35. Xu, X., Hoang, S., Mayo, M. W., and Bekiranov, S. (2010) Application of machine learning methods to histone methylation ChIP-Seq data reveals H4R3me2 globally represses gene expression. *BMC Bioinformatics* **11**, 396
36. Warner, S. M., Hackett, T. L., Shaheen, F., Hallstrand, T. S., Kicic, A., Stick, S. M., *et al.* (2013) Transcription factor p63 regulates key genes and wound repair in human airway epithelial basal cells. *Am. J. Respir. Cell Mol. Biol.* **49**, 978–988
37. Mao, R., Shao, J., Zhu, K., Zhang, Y., Ding, H., Zhang, C., Potent, *et al.* (2017) Selective, and Cell Active Protein Arginine Methyltransferase 5 (PRMT5) inhibitor developed by structure-based virtual screening and hit optimization. *J. Med. Chem.* **60**, 6289–6304
38. Yang, A., Schweitzer, R., Sun, D., Kaghad, M., Walker, N., Bronson, R. T., *et al.* (1999) p63 is essential for regenerative proliferation in limb, craniofacial and epithelial development. *Nature* **398**, 714–718

39. Signoretti, S., Pires, M. M., Lindauer, M., Horner, J. W., Grisanzio, C., Dhar, S., *et al.* (2005) p63 regulates commitment to the prostate cell lineage. *Proc. Natl. Acad. Sci. U. S. A.* **102**, 11355–11360
40. Van Keymeulen, A., Rocha, A. S., Ousset, M., Beck, B., Bouvencourt, G., Rock, J., *et al.* (2011) Distinct stem cells contribute to mammary gland development and maintenance. *Nature* **479**, 189–193
41. Romano, R. A., Smalley, K., Magraw, C., Serna, V. A., Kurita, T., Raghavan, S., *et al.* (2012) ΔNp63 knockout mice reveal its indispensable role as a master regulator of epithelial development and differentiation. *Development* **139**, 772–782
42. Haas, M., Gómez Vázquez, J. L., Sun, D. I., Tran, H. T., Brislinger, M., Tasca, A., *et al.* (2019) ΔN-Tp63 Mediates Wnt/β-Catenin-Induced inhibition of differentiation in basal stem cells of mucociliary epithelia. *Cell Rep* **28**, 3338–3352.e3336
43. Marshall, C. B., Mays, D. J., Beeler, J. S., Rosenbluth, J. M., Boyd, K. L., Santos Guasch, *et al.* (2016) p73 Is Required for Multiciliogenesis and Regulates the Foxj1-Associated Gene Network. *Cell Rep.* **14**, 2289–2300
44. Yang, Y., Riccio, P., Schotsaert, M., Mori, M., Lu, J., Lee, D. K., *et al.* (2018) Spatial-Temporal Lineage Restrictions of Embryonic p63(+) progenitors establish distinct stem cell pools in adult airways. *Dev. Cell* **44**, 752–761.e754
45. Wang, Y., and Tang, N. (2021) The diversity of adult lung epithelial stem cells and their niche in homeostasis and regeneration. *Sci. China Life Sci.* **64**, 2045–2059
46. Rock, J. R., Onaitis, M. W., Rawlins, E. L., Lu, Y., Clark, C. P., Xue, Y., *et al.* (2009) Basal cells as stem cells of the mouse trachea and human airway epithelium. *Proc. Natl. Acad. Sci. U. S. A.* **106**, 12771–12775
47. Zuo, W., Zhang, T., Wu, D. Z., Guan, S. P., Liew, A. A., Yamamoto, Y., *et al.* (2015) p63(+)Krt5(+) distal airway stem cells are essential for lung regeneration. *Nature* **517**, 616–620
48. Zhou, Y., Wang, Y., Li, D., Zhang, T., Ma, Y., and Zuo, W. (2021) Stable long-term culture of human distal airway stem cells for transplantation. *Stem Cells Int.* **2021**, 9974635
49. Huang, H., Fang, Y., Jiang, M., Zhang, Y., Biermann, J., Melms, J. C., *et al.* (2022) Contribution of Trp63(CreERT2)-labeled cells to alveolar regeneration is independent of tuft cells. *Elife* **11**, e78217
50. Zhou, Y., Yang, Y., Guo, L., Qian, J., Ge, J., Sinner, D., *et al.* (2022) Airway basal cells show regionally distinct potential to undergo metaplastic differentiation. *Elife* **11**, e80083
51. Pang, Q., Liu, C., Qiao, Y., Zhao, J., Lam, S. M., Mei, M., *et al.* (2022) GM130 regulates pulmonary surfactant protein secretion in alveolar type II cells. *Sci. China Life Sci* **65**, 193–205
52. Engler, A. E., Mostoslavsky, G., Miller, L., and Rock, J. R. (2019) Isolation, maintenance and differentiation of primary tracheal basal cells from adult rhesus macaque. *Methods Protoc.* **2**, 79
53. Zhi, M., Zhang, J., Tang, Q., Yu, D., Gao, S., Gao, D., *et al.* (2022) Generation and characterization of stable pig pregastrulation epiblast stem cell lines. *Cell Res.* **32**, 383–400
54. Wang, M., Xu, Y., Zhang, Y., Chen, Y., Chang, G., An, G., *et al.* (2021) Deciphering the autophagy regulatory network via single-cell transcriptome analysis reveals a requirement for autophagy homeostasis in spermatogenesis. *Theranostics* **11**, 5010–5027
55. He, H., Chen, J., Zhao, J., Zhang, P., Qiao, Y., Wan, H., *et al.* (2021) PRMT7 targets of Foxm1 controls alveolar myofibroblast proliferation and differentiation during alveologenesis. *Cell Death Dis.* **12**, 841